Inorganica Chimica Acta, 33 (1979) 137–144

The Mössbauer Recoil-Free Fraction and Structure. Part. 1. α, β, γ, δ-Tetraphenylporphinatodihydroxytin(IV)-bis(chloroform)–bis(carbon tetrachloride) Solvate

PHILIP G. HARRISON*, KIERAN MOLLOY** and EDWARD W. THORNTON***

Department of Chemistry, University of Nottingham, University Park, Nottingham NG7 2RD, U.K.

Received August 29, 1978

The structure of α, β, γ, δ-tetraphenylporphinatodihydroxytin(IV) ($TPPSn(OH)_2$) has been determined as its bis(chloroform)–bis(carbon tetrachloride) solvate by Patterson and Fourier techniques to a final 'R'-factor of 15.14% for 4380 independent reflections. Purple crystals of the material are triclinic, space group P1, with a = *12.229(6),* b = *12.310(9),* c = *9.592(8)* Å, α = *102.58(1),* β = *109.64(5),* γ = *91.78(8)°, and are composed of stacks of non-interacting $TPPSn(OH)_2$ molecules, with the solvate molecules occupying spaces in the lattice. The geometry at the tin is only slightly distorted from regular octahedral, with Sn–N bonds of normal length (2.09(5) Å), but with very short bonds to oxygen (2.00(3) and 2.03(5) Å). Tin-119 Mössbauer resonance area data have been collected in the temperature range 77 ⩽ T ⩽ 153 K, and a semi-logarithmic plot of resonance area* versus *temperature is linear in this temperature range, yielding values of the logarithmic temperature coefficient of the recoil-free fraction,* a, *and of the characteristic Mössbauer temperature, θ_M, of $-0.01193\ K^{-1}$ and 122.3 K, respectively. The data have also been used to evaluate the isotropic mean-square amplitudes of vibration, $\langle x_{iso}(T)^2 \rangle$, of the tin atom, normalised to the value at 298 K available from the crystallographic study, in the same temperature range. Root-mean-square values of the vibrational amplitude range from 0.125 Å at 77 K to 0.148 Å at 153 K. From the Goldanskii–Karyagin effect data, it was concluded that the sign of the electric field gradient, V_{zz}, assumed to be coincident with the pseudo-four-fold axis of the molecule, is negative, and that the tin atom vibrates with greater amplitude in the plane of the porphyrin residue (perpendicular to V_{zz}). The temperature coefficient of the root-mean-square amplitude of vibration is significantly larger in the out-of-plane direction (along the O–Sn–O axis) (4.184×10^{-4} Å K^{-1}) than in the in-plane direction (2.618×10^{-4} Å K^{-1}), reflecting the constraining nature of the porphyrin residue. Absolute values of the recoil-free fraction, f_a, were estimated to be 0.100 at 77 K reducing to 0.0404 at 153 K.*

Introduction

Studies of tetrapyrrole derivatives of tin are important because they represent one of the possible ways in which tin may be incorporated into biological systems. Burnham and Zuckerman [1] have demonstrated that tin (as tin(II) chloride) is incorporated into the porphyrin residue via the initial formation of a "sitting-atop" complex in which the bivalent tin atom, which is too large to fit into the cavity of the porphyrin, is bonded to the four nitrogen atoms of the ring system in a square-pyramidal fashion, before oxidation to the smaller higher valence state, which fits the cavity comfortably. The structure of an analogous "sitting-atop" complex, phthalocyaninatotin(II), has been confirmed by crystallography [2], as has the octahedral coordination of the tin(IV) atom in phthalocyaninato [3] and porphinato-tin(IV) [4, 5] derivatives.

Whilst the Mössbauer spectra of most complexes in which tin is coordinated by six very electronegative ligands consist of a single, fairly sharp (Γ is generally ⩽1 mm s^{-1}), both phthalocyaninato [6] and porphinato-tin(IV) [7] complexes exhibit small, but clearly resolvable, quadrupole splittings, and, in the case of the latter, a distinct asymmetry in the intensities of the higher and lower energy lines (Goldanskii–Karyagin effect) [8, 9]. In this Paper, we report the results of an X-ray diffraction study of α, β, γ, δ-tetraphenylporphinatodihydroxytin(IV) (as its bis(chloroform)–bis(carbon tetrachloride) solvate), as well as a study of thermal motion of the tin atom (as probed by a study of the Mössbauer recoil-free fraction and Goldanskii–Karyagin effect).

*Author to whom enquires should be addressed at University of Nottingham.

**Present address: Department of Chemistry, University of Oklahoma, Norman, Oklahoma, U.S.A.

***Present address: Institut für Physikalische Chemie der Universität München, München, West Germany.

Experimental

Crystal Structure Determination

Crystal preparation

A sample of $TPPSn(OH)_2$ was dissolved in dry chloroform and the solution placed in a saturated atmosphere of carbon tetrachloride. Slow evaporation of the solvent yielded hard, purple prismatic crystals. One of approximate dimensions 0.4 × 0.3 × 0.3 mm^3 was mounted directly onto a glass fibre and used both for the initial photography and the subsequent intensity data collection.

Crystal data

$C_{48}H_{32}Cl_{14}N_4O_2Sn$, M = 1311.33, Triclinic, space group P1, a = 12.229(6), b = 12.310(9), c = 9.592(8) Å, α = 102.58(1), β = 109.64(5), γ = 91.78(8)°, V = 1318.86 Å^3, Z = 1, F(000) = 652.

Intensity data collection and structure determination

The space group and initial cell parameters were determined from zero- and first-layer Weissenberg photographs obtained by use of a Nonius Weissenberg goniometer. Cell parameters were further refined by least-squares methods from *ca.* 20 reflections. Relative intensities up to θ = 30.0° were collected by use of Mo-K_α radiation (λ = 0.71069 Å) on a Hilger and Watts Y290 four circle diffractometer. Of 4726 reflections measured, 4380 had a corrected count $I < 3\sigma(I)$ and were used for the structure determination and refinement. Intensities were corrected for Lorentz and polarisation effects, but not for absorption.

The positional parameters of the tin atom were obtained from a three-dimensional Patterson synthesis, and were subsequently used to phase the initial structure factor calculation. After two cycles of

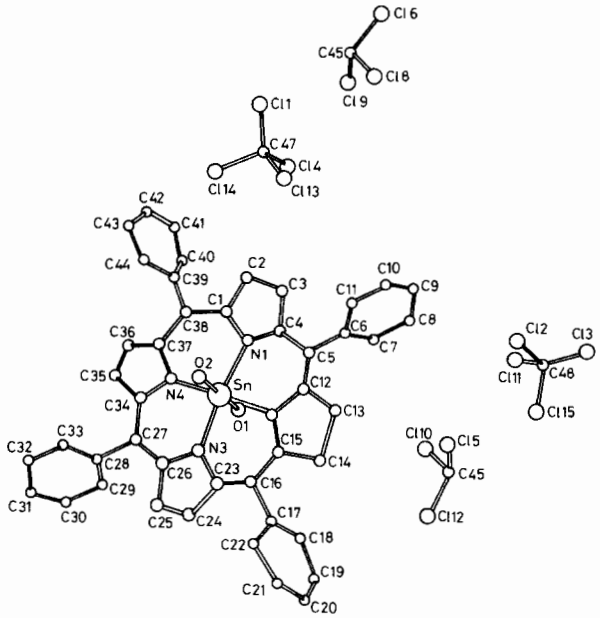

Figure 1. View of the $TPPSn(OH)_2$ molecule showing the atomic numbering. The unlocated carbon atom is shown by a dashed circle.

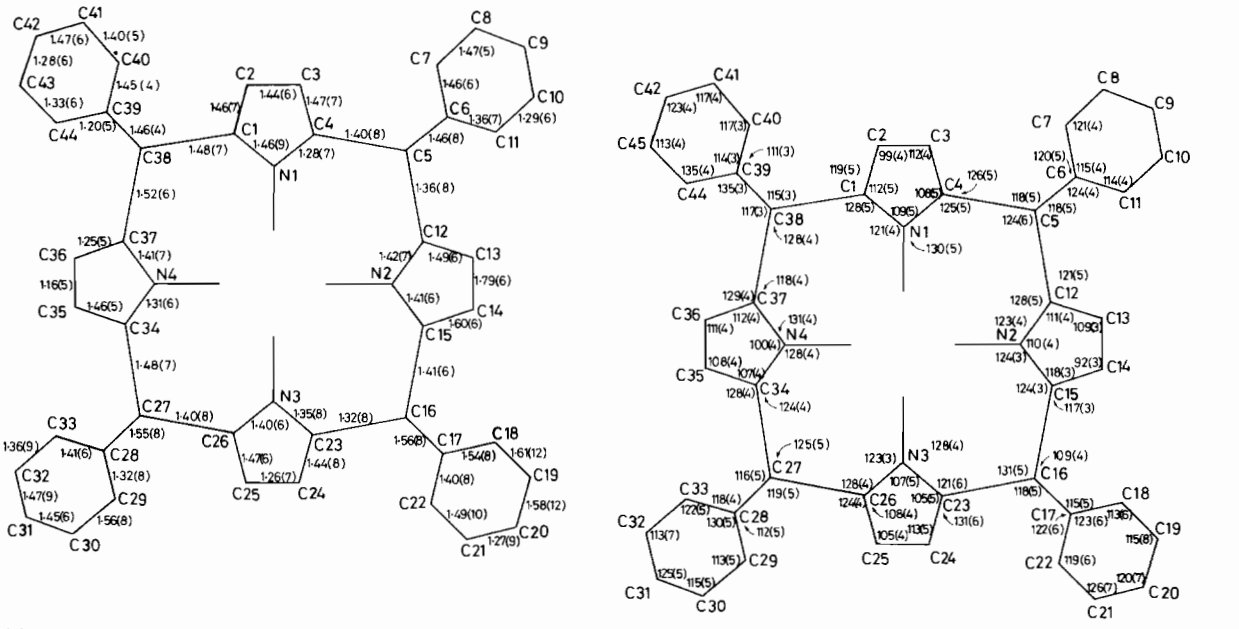

(a) (b)

Figure 2. (a) Bond distances and (b) bond angles in the tetraphenylporphyrin residue (estimated standard deviations are in parentheses).

isotropic least-squares refinement of these, a Fourier synthesis yielded the positions of several light atoms. Alternate cycles of block-diagonal least-squares refinement and (difference) Fourier syntheses ultimately yielded the positions of all the light atoms except for one carbon atom of a phenyl group. After further cycles of isotropic least-squares refinement it was clear that the chloroform and carbon tetrachloride molecules were partially disordered among two sets of sites in the lattice, although one set was far more populated than the other. However, attempts to satisfactorily locate the positions of the second set of solvent molecule positions was unsuccessful, and refinement was finally discontinued when the 'R'-value was 15.14%. Calculations were performed using the CRYSTALS suite of programmes. The scattering factors used were those for neutral atoms [10]. Atomic numbering is illustrated in Fig. 1. Final atomic positions and isotropic thermal parameters are listed in Table I, and bond distance and angle data are given in Table II and Fig. 2.

TABLE I. Final Atomic Positions and Isotropic Thermal Parameters (estimated standard deviations are in parentheses).

Atom	X/A	Y/B	Z/C	U(iso)
Sn(1)	0.0000	0.0000	0.0000	0.0337(6)
O(1)	−0.043(2)	−0.021(2)	0.177(3)	0.035(6)
O(2)	0.036(4)	0.024(4)	−0.184(5)	0.06(1)
N(1)	0.053(5)	0.171(5)	0.107(7)	0.04(2)
C(3)	0.142(4)	0.338(4)	0.251(6)	0.05(1)
C(4)	0.154(3)	0.220(3)	0.195(4)	0.044(6)
C(1)	−0.029(3)	0.254(3)	0.085(4)	0.023(8)
C(2)	0.024(6)	0.364(6)	0.184(8)	0.04(2)
C(38)	−0.156(2)	0.235(2)	0.000(3)	0.026(5)
C(39)	−0.216(4)	0.336(4)	0.004(6)	0.03(1)
C(44)	−0.210(2)	0.419(2)	−0.040(3)	0.039(5)
C(40)	−0.300(3)	0.332(2)	0.079(3)	0.030(6)
C(41)	−0.364(4)	0.424(4)	0.091(6)	0.04(1)
C(43)	−0.253(4)	0.517(4)	−0.021(6)	0.04(1)
C(42)	−0.334(4)	0.517(4)	0.036(6)	0.04(1)
C(37)	−0.229(6)	0.126(6)	−0.104(8)	0.06(2)
N(4)	−0.172(4)	0.029(4)	−0.118(5)	0.04(1)
C(36)	−0.332(3)	0.111(3)	−0.196(4)	0.014(7)
C(34)	−0.261(5)	−0.045(5)	−0.207(6)	0.03(1)
C(35)	−0.360(3)	0.017(3)	−0.259(4)	0.046(7)
C(27)	−0.252(4)	−0.165(3)	−0.263(5)	0.018(9)
C(26)	−0.151(4)	−0.219(3)	−0.213(5)	0.023(9)
N(3)	−0.042(3)	−0.172(3)	−0.104(4)	0.014(8)
C(25)	−0.147(3)	−0.340(3)	−0.263(5)	0.036(9)
C(24)	−0.043(3)	−0.355(3)	−0.193(4)	0.041(7)
C(23)	0.030(4)	−0.252(4)	−0.104(6)	0.03(1)
C(16)	0.138(3)	−0.235(2)	−0.004(4)	0.045(6)
C(17)	0.217(4)	−0.331(4)	−0.013(5)	0.05(1)
C(18)	0.186(3)	−0.431(3)	0.046(4)	0.035(8)
C(19)	0.276(4)	−0.523(4)	0.048(6)	0.06(1)
C(20)	0.35(1)	−0.52(1)	−0.06(1)	0.05(4)
C(21)	0.361(7)	−0.434(7)	−0.106(9)	0.06(2)
C(22)	0.300(4)	−0.333(4)	−0.085(5)	0.068(9)
C(15)	0.208(4)	−0.135(4)	0.087(5)	0.017(9)
N(2)	0.171(4)	−0.028(3)	0.092(5)	0.025(9)
C(12)	0.258(5)	0.054(5)	0.205(7)	0.04(1)
C(13)	0.367(8)	0.003(8)	0.27(1)	0.03(3)
C(14)	0.341(3)	−0.144(3)	0.185(4)	0.078(7)
C(5)	0.254(3)	0.167(3)	0.248(4)	0.054(8)
C(6)	0.361(1)	0.236(1)	0.354(2)	0.032(4)
C(7)	0.382(1)	0.287(1)	0.514(2)	0.034(4)
C(11)	0.443(2)	0.269(2)	0.299(2)	0.059(5)
C(10)	0.549(2)	0.334(2)	0.419(2)	0.054(5)
C(8)	0.477(2)	0.352(2)	0.598(2)	0.049(5)
C(28)	−0.367(2)	−0.237(2)	−0.374(2)	0.044(6)
C(29)	−0.361(2)	−0.278(2)	−0.511(3)	0.064(6)
C(30)	−0.477(2)	−0.347(2)	−0.628(2)	0.065(5)
C(31)	−0.566(2)	−0.366(2)	−0.564(3)	0.030(6)
C(33)	−0.462(1)	−0.245(1)	−0.322(2)	0.036(4)
C(32)	−0.564(2)	−0.309(2)	−0.411(2)	0.066(5)
Cl(1)	0.957(2)	0.177(1)	0.414(2)	0.078(4)
C(47)	0.968(2)	0.288(2)	0.571(3)	0.092(7)
Cl(4)	0.876(2)	0.376(2)	0.466(3)	0.103(5)
Cl(13)	1.090(6)	0.344(6)	0.674(8)	0.11(2)
Cl(14)	0.881(5)	0.238(5)	0.656(7)	0.14(1)
Cl(2)	0.010(7)	0.824(7)	0.565(9)	0.08(2)
O(48)	0.031(6)	0.712(6)	0.445(9)	0.08(2)
Cl(3)	0.118(4)	0.611(4)	0.522(6)	0.10(1)
Cl(11)	−0.108(4)	0.619(4)	0.361(5)	0.10(1)
Cl(15)	0.096(5)	0.746(4)	0.312(6)	0.12(1)
Cl(5)	0.356(5)	0.948(4)	0.839(6)	0.10(1)
C(46)	0.263(6)	1.048(5)	0.753(8)	0.07(1)
Cl(10)	0.346(6)	1.178(5)	0.863(8)	0.12(1)
Cl(12)	0.252(6)	1.021(5)	0.572(8)	0.12(2)
Cl(6)	0.634(4)	0.029(4)	0.112(6)	0.11(1)
C(45)	0.719(6)	−0.047(5)	0.215(8)	0.07(2)
Cl(8)	0.669(4)	−0.184(4)	0.131(6)	0.12(1)
Cl(9)	0.711(5)	−0.025(5)	0.408(7)	0.10(1)

Tin-119 Mössbauer Data

Our Mössbauer spectrometer has been described previously [11]. A sample of the material was finely ground and made up into a disc of density *ca.* 10 mg ^{119}Sn cm^{-2} between aluminium foil windows. Spectra were recorded versus a $Ca^{119}SnO_3$ source (Radiochemical Centre, Amersham) (nominal strength 5 mci) at temperatures between 77 K and 153 K accumulating $\geqslant 10^6$ counts per channel. Data reduction was accomplished by fitting the spectra to Lorentzian line shapes using usual least-squares methods.

Results and Discussion

Structure of the TPPSn(OH)$_2$–Chloroform/Carbon Tetrachloride Solvate

Crystals of the material are composed of stacks of individual non-interacting $TPPSn(OH)_2$ molecules with the chlorinated hydrocarbon solvent molecules

TABLE II. Bond Distances (Å) and Angles (degrees) of Atoms Bonded to Tin.[a]

Bond Distances:	
Sn–O(1)	2.00(3)
Sn–O(2)	2.03$_5$(5)
Sn–N(1)	2.10(6)
Sn–N(2)	2.04$_5$(5)
Sn–N(3)	2.10(5)
Sn–N(4)	2.11(5)
Bond Angles:	
O(1)–Sn–O(2)	177(2)
O(1)–Sn–N(1)	90(2)
O(1)–Sn–N(2)	95(2)
O(1)–Sn–N(3)	91(2)
O(1)–Sn–N(4)	91(2)
O(2)–Sn–N(1)	89(2)
O(2)–Sn–N(2)	88(2)
O(2)–Sn–N(3)	90(2)
O(2)–Sn–N(4)	86(2)
N(1)–Sn–N(2)	88(2)
N(1)–Sn–N(3)	177(3)
N(1)–Sn–N(4)	93(2)
N(2)–Sn–N(3)	89(2)
N(2)–Sn–N(4)	173(3)
N(3)–Sn–N(4)	90(2)

[a]Estimated standard deviations are in parentheses.

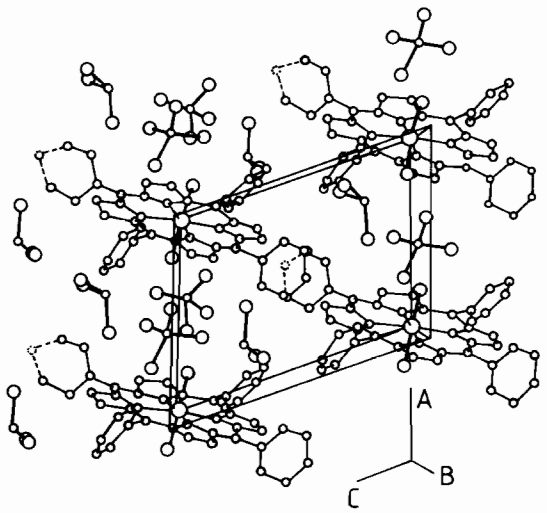

Figure 3. Unit cell projection of $TPPSn(OH)_2 \cdot 2CHCl_3 \cdot 2CCl_4$ showing the disposition of the solvate molecules.

occupying spaces in the lattice (Fig. 3). The general features of the $TPPSn(OH)_2$ molecule resemble closely those of $TPPSnCl_2$ [4], although in the present case the rather poor quality of the data gives rise to undesirably large standard deviations in the positions of the peripheral atoms of the tetraphenylporphyrin residue. As expected, the tin atom is coplanar with the porphyrin skeleton, as may be seen from the

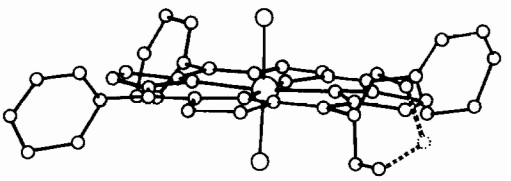

Figure 4. Perspective view of the $TPPSn(OH)_2$ molecule showing the 'paddle-wheel' orientation of the four phenyl groups relative to the plane of the porphyrin residue.

perspective view of the molecule shown in Fig. 4. The porphyrin macrocycles in $TPPSnCl_2$ [4] and $OEPSnCl_2$ [5] (OEP = 1, 2, 3, 4, 5, 6, 7, 8-octaethylporphinato) are also planar, but in the analogous phthalocyaninatodichlorotin(IV) ($PcSnCl_2$) [3] the macrocycle experiences a "stepped" deformation in which the plane of one half of the macrocycle is *ca.* 0.76 Å above the plane of the other. The octahedral geometry of the tin atom is, however, preserved. As in $TPPSnCl_2$ [4], the four phenyl rings in $TPPSn(OH)_2$ are almost orthogonal to the plane of the porphinato residue (Fig. 4).

The tin atom is octahedrally coordinated by the four pyrrollic nitrogen atoms and the two hydroxyl groups, which occupy axial coordination sites (Fig. 1). The tin–nitrogen bond distances (mean 2.09(5) Å) are comparable with those observed for $PcSnCl_2$ [3] (2.051(3) Å), $OEPSnCl_2$ [5], (2.093(6) Å), and $TPPSnCl_2$ [4] (2.098(2) Å), but the tin–oxygen bonds are very short (2.00(3) and 2.035(5) Å), being shorter even than the Sn^{IV}–O bond distances in $[Sn^{IV}Sn^{II}(O_2CC_6H_4NO_2\text{-}o)_4O \cdot THF]_2$ [12] (shortest 2.047(6) Å, mean 2.059(8) Å) and $(SnCl_3OH.H_2O)_2 \cdot 3THF$ [13] (2.05(3), 2.06(3), 2.10(3) Å). The octahedral geometry about tin is essentially regular with the mean $\widehat{OSnN}$ bond angle 90(2)° and the $\widehat{OSnO}$ angle 177(2)°.

Tin-119 Mössbauer Recoil-free Fraction Studies

Experimental isomer shift, quadrupole splitting, and resonance area data for several temperatures in the range $77 \leqslant T \leqslant 153$ K are listed in Table III. Both the isomer shift and quadrupole splitting are constant within experimental error in this temperature range. However, the total resonance area and the area ratio of the two component wings of the doublet vary substantially with temperature. A semi-logarithmic plot of the total resonance area, $A(T)_{total}$, *versus* temperature, T, is shown in Fig. 5, and is linear over the observed temperature range. Since, in the thin absorber approximation, the total resonance area, A(T), is directly proportional to the absorber recoil-free fraction, $f_a(T)$, this type of behaviour is consonant with that expected from the application of the Debye model in the high-temperature limit ($T \geqslant \theta_D/2$, θ_D = Debye temperature) (albeit for an ideal, isotropic cubic solid). Nevertheless, using this model we have

TABLE III. Mössbauer Data for $TPPSn(OH)_2 \cdot 2CHCl_3 \cdot 2CCl_4$.

Temperature (K)	I.S.[a–c]	Q.S.[a,c]	Γ_-[a]	Γ_+[a]	A_-	A_+	A_{total}	A_+/A_-
77	0.07	0.66	0.892	1.035	2.357	3.475	5.832	1.474
88	0.07	0.66	0.790	1.017	2.055	2.977	5.032	1.448
100	0.08	0.65	0.794	0.911	1.820	2.429	4.250	1.335
109	0.07	0.66	0.785	0.928	1.605	2.163	3.768	1.348
122	0.09	0.65	0.873	0.931	(1.591)[d]	(1.740)[d]	3.331	(1.094)[d]
132	0.04	0.62	0.876	1.010	1.214	1.877	3.092	1.546
142	0.01	0.65	0.756	0.975	1.006	1.600	2.606	1.590
153	0.05	0.66	0.830	0.985	0.972	1.349	2.321	1.388

[a]mm s^{-1}. [b]Relative to $CaSnO_3$ (=0). [c]Isomer shifts are accurate to at least ±0.03 mm s^{-1}, quadrupole splittings to at least ±0.06 mm s^{-1}. [d]These values are obviously erroneous and result from an inaccurate resolution of the total resonance envelope into its two components. The value for $A_{total}(122)$ is consistent with the other data.

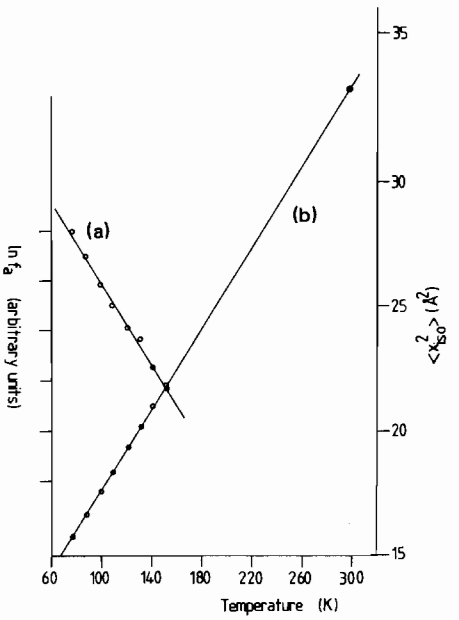

Figure 5. Plots of (a) $\ln f_a$ *versus* T and (b) $\langle x_{iso} \rangle$ *versus* T. The latter plot has been normalised to the room temperature crystallographic datum point (●).

$$A(T) \propto f_a(T) = \exp - \left[\frac{6 E_R T}{k \theta_M^2} \right] \quad (1)$$

where E_R is the recoil energy of the Mössbauer nuclide, k the Boltzmann constant, and θ_M the characteristic Mössbauer temperature of the material (equivalent to θ_D in the ideal case). Therefore, the logarithmic temperature coefficient of the recoil-free fraction, a, is given by

$$a = \frac{d}{dT} [\ln f_a(T)] = \frac{d}{dT} [\ln A(T)] = - \frac{6 E_R}{k \theta_M^2} \quad (2)$$

In the present case, $a = -0.01193\ K^{-1}$, from which θ_M is evaluated to be 122.3 K, a value which compares well with that deduced for the octahedrally coordinated tin(IV) atoms in $[Sn^{IV}Sn^{II}(O_2CC_6H_4\text{-}NO_2\text{-}o)_4O \cdot THF]_2$ [12].

The absorber recoil-free fraction $f_a(T)$, is also related to the mean-square amplitude of vibration, $\langle x_{iso}(T)^2 \rangle$, of the Mössbauer nuclide by

$$f_a(T) = \exp [-\langle x_{iso}(T)^2 \rangle / \lambda\!\!\!^{-2}] \quad (3)$$

where $\lambda\!\!\!^{-}$ is the wavelength (divided by 2π) of the Mössbauer transition, and therefore

$$a = \frac{d}{dT} [\ln f_a(T)] = - \frac{1}{\lambda\!\!\!^{-2}} \frac{d}{dT} \langle x_{iso}(T)^2 \rangle \quad (4)$$

The variation with temperature of the mean-square amplitude of vibration $\langle x_{iso}(T)^2 \rangle$ in the same temperature range, normalised to the value at 298 K derived from the crystallographic thermal parameter is also shown in Fig. 5. Again the plot is linear, with a temperature coefficient of 8.14×10^{-5} Å^2 K^{-1} and intercept 9.44×10^{-3} Å^2. Thus, at 77 K the root-mean-square amplitude of vibration of the tin atom is reduced to 0.125 Å, compared with values of 0.148 Å at 153 K, and 0.184 Å at 298 K. Furthermore, since equation (3) holds for any temperature, the use of the crystallographic datum to normalise the data allows the estimation of *absolute* values of the recoil-free fraction. Thus, at 77 K, f_a = 0.100, decreasing to 0.0404 at 153 K, and to an extrapolated value of 0.0072 at 298 K, less than 1% of the value at 77 K.

As may be seen from the data in Table III and from the sample spectrum depicted in Fig. 6, the two components of the quadrupole split doublet are not of equal intensity, even though the sample was very finely ground in order to eliminate orientation effects. This inequality of intensity, known as the Goldanskii–Karyagin effect [8, 9], arises from the vibrational anisotropy of the Mössbauer nuclide.

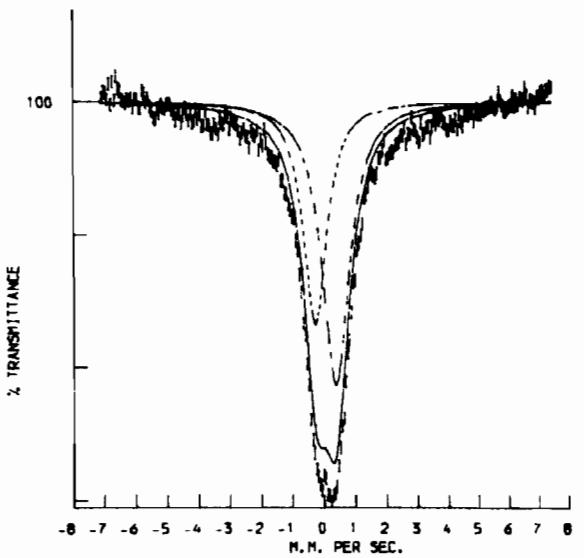

Figure 6. The Mössbauer spectrum of $TPPSn(OH)_2 \cdot 2CHCl_3 \cdot 2CCl_4$ at 77 K. Curve-fitted peaks are shown as dashed (individual peaks) and solid (total envelope) lines.

Thus, assuming axial symmetry of the electric field gradient, the ratio of the line intensities, R, is given by

$$R = \frac{A_1}{A_2} = \frac{\int_0^{\pi} (\exp - \epsilon \cos^2\theta)(1 + \cos^2\theta) \sin\theta \, d\theta}{\int_0^{\pi} (\exp - \epsilon \cos^2\theta)(\tfrac{5}{3} - \cos^2\theta) \sin\theta \, d\theta} \quad (5)$$

where A_1 and A_2 refer to the intensities of the $(\pm\frac{1}{2} \longleftrightarrow \pm\frac{3}{2})$ and $(\pm\frac{1}{2} \longleftrightarrow \pm\frac{1}{2})$ transitions, respectively, and ϵ is defined as

$$\epsilon = \left(\frac{1}{\lambda^2}\right) [\langle x_{\parallel}^2 \rangle - \langle x_{\perp}^2 \rangle] \quad (6)$$

where the subscripts $\parallel$ and $\perp$ refer to vibrations parallel and perpendicular to the principal axis. We have evaluated the two integrals in the expression for R in equation (5) above; however, a correct interpretation of the intensity ratio data is dependent upon a knowledge of the sign of the electric field gradient, V_{zz}, at the Mössbauer nuclide. For tin-119, the nuclear quadrupole moment, eQ, is negative, and therefore for an oblate field V_{zz} is positive, and the $\pm\frac{3}{2}$ level moves to lower energy, whilst for a prolate field V_{zz} is negative, and the $\pm\frac{1}{2}$ level is at lower energy. In the absence of an independent determination of the sign of V_{zz} by analysis of a magnetically perturbed spectrum, the sign may be deduced by a careful examination of the Goldanskii–Karyagin effect data. If the $\pm\frac{3}{2}$ level lies at lower energy (*i.e.* an oblate field and V_{zz} positive), then $R = I_-/I_+$ (where I_+ is the intensity of the higher velocity line, and I_- that of the lower velocity line). This, however, leads to unacceptably high values of $\epsilon\lambda^2$ (in some cases in excess of 0.068 Å^2). On the other hand, if the $\pm\frac{1}{2}$ level lies at lower energy (*i.e.* a prolate field and V_{zz} negative), then $R = I_+/I_-$. In the case of $TPPSn(OH)_2$, it is reasonable to assume that V_{zz} lies along the pseudo-four-fold axis collinear with the O–Sn–O axis,with therefore a greater concentration of electron density in the bonds to oxygen than those to nitrogen. Values of $\epsilon\lambda^2$ so determined are negative (Table IV), indicating that the tin atom is vibrating with greater amplitude in the plane of the porphyrin residue (perpendicular to V_{zz}) than along the O–Sn–O axis (parallel to V_{zz}). This result may at first seem to be at variance with the crystallographic [4] and Goldanskii–Karyagin [7] data for the analogous $TPPSnCl_2$. The values of $\epsilon\lambda^2$ at room temperature derived from the X-ray data is +0.013 Å^2, whilst at 80 K the Goldanskii–Karyagin ratio yields a value of +0.026 Å^2 (assuming V_{zz} is negative [15]), *i.e.* the tin atom is vibrating with larger amplitude parallel to the principal (Cl–Sn–Cl) axis than perpendicular to it (in the plane of the porphyrin residue). However, examination of the relevant bond distances shows that, whilst the Sn–N bond distances are similar in both compounds (*vide supra*), the Sn–Cl bond distances are long (2.420(1) Å) [4], whilst the Sn–O bond distances are exceptionally short, and shorter than the Sn–N bond distances. It is, therefore, clear that the tin atom vibrates with greater amplitude in the direction in which the bonded atoms are the more distant.

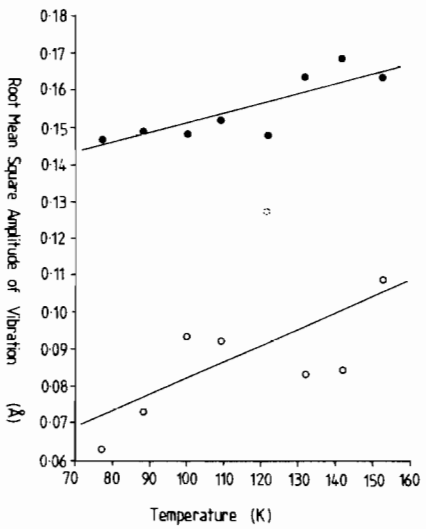

Figure 7. Plots of the root-mean-square amplitudes of vibration parallel (○) and perpendicular (●) to the pseudo-four-fold molecular axis *versus* T.

TABLE IV. Mean-square and Root-mean-square Amplitude Data for $TPPSn(OH)_2 \cdot 2CHCl_3 \cdot 2CCl_4$.

Temperature (K)	$-\epsilon\lambda^2$ (a)	$\langle x^2_{iso} \rangle$ (a, b)	$\langle x^2_{\parallel} \rangle$ (a)	$\langle x^2_{\perp} \rangle$ (a)	$\langle x^2_{\parallel} \rangle^{1/2}$ (c)	$\langle x^2_{\perp} \rangle^{1/2}$ (c)
77	1.767	1.571	0.393	2.16	0.627	1.47
88	1.685	1.660	0.537	2.22	0.733	1.49
100	1.324	1.758	0.875	2.20	0.936	1.48
109	1.467	1.831	0.853	2.32	0.924	1.52
122	(0.437)	1.937	(1.646)	(2.08)	(1.283)	(1.44)
132	1.992	2.018	0.690	2.68	0.831	1.64
142	2.129	2.100	0.714	2.84	0.845	1.69
153	1.501	2.189	1.188	2.69	1.089	1.64
298		3.365[d]				

(a) These values have been multiplied by 10^2 (Å). (b) Derived from $\langle x_{iso}(T)^2 \rangle = 8.14 \times 10^{-5} T + 9.44 \times 10^{-5}$. (c) These values have been multiplied by 10 (Å). (d) From X-ray data.

Replacement of the isotropic mean-square amplitude term, $\langle x^2_{iso} \rangle$, by the expression $\frac{1}{3}[2\langle x^2_{\perp} \rangle + \langle x^2_{\parallel} \rangle]$, absolute root-mean-square amplitudes of vibration parallel and perpendicular to the principal axis may be evaluated. These are summarised in Table IV and plotted graphically in Fig. 7. From the latter, it can be seen that the in-plane root-mean-square amplitude, $\langle x^2_{\perp} \rangle^{1/2}$, over the temperature range $77 \geqslant T \leqslant 153$ K, although the latter exhibits a significantly larger temperature coefficient (2.618×10^{-4} Å K^{-1} *versus* 4.184×10^{-4} Å K^{-1}), the range of values for the in-plane amplitude (~0.145–0.176 Å) compares favourably with that deduced from the X-ray data for $TPPSnCl_2$ (0.153 Å) at ambient temperature [4]. In contrast, the out-of-plane amplitude is much smaller over the same temperature range (~0.063–0.109 Å). The larger temperature coefficient of the out-of-plane amplitude, therefore, reflects the constraining nature of the porphyrin residue upon the thermal excitation of the tin atom compared with the easily translated hydroxyl groups of the axial coordination positions.

Acknowledgements

We thank the Science Research Council for the award of a Research Grant (to P. G. H.) and a Research Studentship (to K. M.) , Dr. J. C. Pommier and Dr. J. R. Richards of the University of Bordeaux I for the sample of $TPPSn(OH)_2$, and Professor T. J. King for recording the intensity data.

References

1 B. F. Burnham and J. J. Zuckelman, *J. Am. Chem. Soc. 92,* 1547 (1970).
2 M. K. Friedel, B. F. Hoskins, R. L. Martin and S. A. Mason, *Chem. Commun.*, 400 (1970).
3 D. Rodgers and R. S. Osborn, *Chem. Commun.*, 840 (1971).
4 D. M. Collins, W. R. Scheidt and J. L. Hoard, *J. Am. Chem. Soc., 94,* 6689 (1972).
5 D. L. Cullen and E. L. Meyer, *Acta Cryst., B29,* 2507 (1973).
6 M. O'Rourke and C. Curran, *J. Am. Chem. Soc., 92,* 1501 (1970).
7 N. W. G. Debye and A. D. Adler, *Inorg. Chem., 13,* 3037 (1974).
8 V. I. Goldanskii, G. M. Gorodinskii, S. V. Karyagin, L. A. Kovytko, L. M. Krizhanskii, E. F. Makarov, I. P. Suzdalev and V. V. Khrapov, *Dokl. Akad. Nauk SSSR, 147,* 127 (1962).
9 S. V. Karyagin, *Dokl. Akad. Nauk SSSR, 148,* 1102 (1963).
10 'International Tables for Z-ray Crystallography', vol. III, Kynoch Press, Birmingham (1962).
11 C. C. Addison, P. G. Harrison, N. Logan, L. Blackwell and D. H. Jones, *J. Chem. Soc. Dalton,* 830 (1975).
12 P. F. R. Ewings, P. G. Harrison, A. Morris and T. J. King, *J. Chem. Soc. Dalton,* 1602 (1976).
13 N. G. Bokii and Yu. T. Struchkov, *J. Struct. Chem., 12,* 253 (1971).
14 " The Mössbauer Effect and its Application to Chemistry", V. I. Goldanskii, Van Nostrand (1966).
15 The assumption that V_{zz} is positive leads to a value of $\epsilon\lambda^2$ of -0.014 Å^2, *i.e.* that the tin atom vibrates with larger amplitude in the plane of the porphyrin residue, which is contrary to the X-ray crystallographic data at ambient temperature.